



Matthews, J., Wright, M., Clarke, D., Morley, E., Silva, H. G., Bennett, A., Robert, D., & Shallcross, D. (2019). Urban and rural measurements of atmospheric potential gradient. *Journal of Electrostatics*, 97, 42-50. <https://doi.org/10.1016/j.elstat.2018.11.006>

Peer reviewed version

License (if available):  
CC BY-NC-ND

Link to published version (if available):  
[10.1016/j.elstat.2018.11.006](https://doi.org/10.1016/j.elstat.2018.11.006)

[Link to publication record in Explore Bristol Research](#)  
PDF-document

This is the author accepted manuscript (AAM). The final published version (version of record) is available online via Elsevier at <https://doi.org/10.1016/j.elstat.2018.11.006> . Please refer to any applicable terms of use of the publisher.

## University of Bristol - Explore Bristol Research

### General rights

This document is made available in accordance with publisher policies. Please cite only the published version using the reference above. Full terms of use are available: <http://www.bristol.ac.uk/red/research-policy/pure/user-guides/ebr-terms/>

1 **Urban and rural measurements of atmospheric potential**  
2 **gradient**

3

4 **J C Matthews<sup>1</sup>, M D Wright<sup>1</sup>, D Clarke<sup>2</sup>, E L Morley<sup>2</sup>, H Silva<sup>3,4</sup>, A J Bennett<sup>5,6</sup>, D Robert<sup>2</sup>, D E**  
5 **Shallcross<sup>1</sup>**

6

7 1 School of Chemistry, University of Bristol, Cantock's Close, Bristol, BS8 1TS, UK

8 2 School of Biological Sciences, Life Sciences Building, University of Bristol, 24 Tyndall Avenue,  
9 Bristol, BS8 1TQ, UK.

10 3 Renewable Energies Chair, University of Évora, IIFA, Palácio do Vimioso, Largo Marquês de  
11 Marialva, Apart. 94, 7002-554, Évora, Portugal.

12 4 Earth Sciences Institute, University of Évora, Rua Romão Ramalho, 59, 7000-671, Évora, Portugal.5

13 5 Bristol Industrial and Research Associates Limited (Biral), P O Box 2, Portishead, Bristol, BS20 7JB,  
14 UK

15 6 Department of Electronic and Electrical Engineering, University of Bath, Bath, BA2 7AY, UK

16

17 E-mail: [j.c.matthews@bristol.ac.uk](mailto:j.c.matthews@bristol.ac.uk)

18

19 Declarations of interest: none

20 **Abstract**

21

22 Atmospheric potential gradient was measured at three sites within the Bristol area of the UK  
23 between 19th May and 24th June 2016. Two sites were on rooftops within the city of Bristol,  
24 800 m apart from each other, while the third was in a rural location 17 km to the south.  
25 Potential gradient measurements at the two rooftop urban sites showed great temporal  
26 similarity, implying that a rooftop measurement may be assumed to represent the local urban  
27 area. Frequency domain analysis indicated a half-day cycle in the urban sites that was not  
28 observed in the rural site, consistent with other studies showing the effect of traffic aerosol  
29 on potential gradient measurements. The correlation between the two urban sites was not  
30 affected by an increase in aerosol concentration. Removal of data during rainfall, as well as  
31 one hour before and after rain removed some of the larger changes in potential gradient  
32 typical of disturbed weather. However, large changes of potential gradient still existed,  
33 showing that rainfall alone should not be relied upon as an indicator of a non-fair weather  
34 potential gradient.

35

36

37 **Keywords**

38

39 Atmospheric electricity, aerosol, urban environment, disturbed weather

40

## 41        **1. Introduction**

42

43    The Atmospheric Potential Gradient (PG) is the vertical electric field present in the  
44    atmosphere, with positive values indicating a downward pointing field. The PG is an  
45    atmospheric measurement that has been recorded through recent history and is now  
46    becoming more common as modern field mill designs enable continuous robust  
47    measurements in many different environments. These measurements have been used to  
48    infer presence and physical characteristics of aerosols [1, 2], and the passage of smoke in  
49    historical data [3, 4]. PG has been used to measure meteorological phenomena and the  
50    passage of charged plumes overhead [5, 6]. Current research on the electrosensitivity of  
51    insects and spiders require an understanding of the local PG to better understand animal  
52    behaviour [7, 8].

53    The global background PG is a consequence of the Earth's electrical circuit which is generated  
54    by thunderstorm activity throughout the globe [9, 10]; thunderstorms transfer charge from  
55    the ground to the ionosphere, which is maintained at a high potential ( $\sim 2.4 \times 10^5$  V) [11]. This  
56    charge transfers back to ground through an atmosphere that is weakly conducting due to the  
57    presence of atmospheric ions created by cosmic and solar rays and (closer to the surface) by  
58    ground based radiation. Whilst the vertical current density flowing between the ionosphere  
59    and surface is small, of order  $10^{-12}$  Am<sup>-2</sup> [11], this current produces an appreciable potential  
60    gradient of  $\sim 100$  Vm<sup>-1</sup> near the surface due to its flow through the extremely low conductivity  
61    air. The global background PG has a 24 hour cycle, caused by the daily variation of  
62    thunderstorm and shower cloud activity throughout the globe and therefore ionospheric  
63    potential [9]. This cycle was found by averaging the diurnal cycle of PG measured on the  
64    research ship Carnegie in a series of cruises between 1909 and 1929 [12]. This variation is not  
65    usually seen in urban fields as local sources can mask it.

66    On a regional scale, charged rain clouds and precipitation cause large fluctuations to the  
67    global background PG to such an extent that analysis of PG with a view to global processes is  
68    often constrained to fair weather measurements, though the definition of fair weather can  
69    vary it is typically described by a clear sky, low wind speeds and no precipitation [13]. Locally,  
70    sources of space charge (splashing water, power lines, combustion sources) can cause  
71    changes in PG through Coulomb fields [14-16], and sources of aerosol can cause a reduction

72 in atmospheric conductivity locally through attachment of ions to aerosols, and hence  
73 increase the local field as a consequence of Ohm's law [3, 17].

74 Within an urban environment, there is an increased aerosol content which can affect levels  
75 of PG [18], and therefore it is important to be able to discern the effects of local sources on  
76 the PG time series recorded. Analysis from two measurement positions in a city will allow the  
77 extent of local PG disruption to be viewed, and a comparison to a third rural site will give an  
78 indication of how the city environment can disrupt the field. The early results presented here  
79 seek to prove the value of measuring PG in a city, and will help to interpret further results  
80 from urban sites.

### 81 *1.1 Global factors affecting atmospheric PG*

82 The amount of ionisation that occurs in the atmosphere is dependent on the amount and  
83 penetration of galactic cosmic rays. As the solar-magnetic and geomagnetic fields give a level  
84 of shielding to cosmic rays, there is an effect of the Sun's activity on the Earth's electric field  
85 due to decreased shielding of cosmic rays. This is shown by an 11-year cycle, corresponding  
86 to solar activity, in the global electric circuit [19]. In addition, cosmic ray events and solar  
87 events have also been shown to affect the Earth's circuit [20]. Thunderstorms are the main  
88 driver of the atmospheric electric field, changes in potential across a thundercloud caused by  
89 internal processes cause electrical breakdown across clouds or towards the ground. Ground  
90 strikes from thunderstorms, breakdown events and currents above and below clouds are  
91 what cause charge to be transferred to the ionosphere. The global electrical circuit is  
92 completed by the air-Earth current carried by charge carriers in the atmosphere transferring  
93 charge back to ground and maintaining the ionospheric potential [19].

### 94 *1.2 Regional factors affecting atmospheric PG*

95 Regionally, the global electric field is affected by the local weather; thunderstorms are the  
96 most dramatic of examples, but rainclouds and fog also affect the value of PG measured at  
97 the ground [22]. Fog has a large effect on the local PG; Piper and Bennett [5] demonstrate a  
98 change in PG during a fog and mist event, with an increase in PG when fog begins, and an  
99 increase in variability as the fog begins to dissipate.

100 Many measurements of atmospheric PG around the globe, including measurements  
101 presented here from Bristol, are now being collected as part of the Global Co-ordination of  
102 Atmospheric Electricity Measurements (GloCAEM; <https://glocaem.wordpress.com/>). This  
103 will better enable regional differences and the global nature of the atmospheric electric circuit  
104 to be explored.

105

### 106 *1.3 Local sources of space charge affecting atmospheric PG*

107 Local sources of PG can cause large changes in atmospheric PG over a short distance.  
108 Atmospheric ions produced by high voltage power lines can remain aloft in the air, attaching  
109 to aerosols, and cause large perturbations to the PG when compared with measurements  
110 made upwind [15, 23]. Splashing water can create space charge [24, 14]. Near a lake in  
111 Portugal, PG measurements were used to elucidate space charge caused by breaking water,  
112 as well as the convective effect of the so-called 'lake breeze' which acted to remove aerosol  
113 and transport freshly created ions over the measurement sites [25]. Traffic can produce highly  
114 charged particles due to combustion processes in the engine [16, 26].

### 115 *1.4 Local effects of aerosol on atmospheric PG*

116 Successful attempts have been made to infer the presence of pollutants from historic PG  
117 measurements. Harrison [4] used atmospheric conductivity and PG measurements to infer  
118 smoke levels; assuming that increases in PG were caused by decreased atmospheric  
119 conductivity due to attachment of ions to smoke particles, testing the method when smoke  
120 concentrations were known. The technique proved effective in estimating smoke  
121 concentrations from London at Kew. Using a similar approach, levels of pollution from  
122 Glasgow and the surrounding area were determined from measurements of PG undertaken  
123 at multiple points in Scotland by Lord Kelvin and by applying plume dynamics [3]. Dust  
124 particles in air can also self-generate charge, and the passage of Saharan dust and Iberian  
125 smoke carried aloft over the UK was detected by a change in PG measured in Reading,  
126 Chilbolton and in Bristol [6], and charged dust overhead has been detected using arrays of  
127 field mills in Portugal [27]. Both examples demonstrate the advantage of using more than one  
128 PG measurement site.

129 Urban measurements of PG using a Bendorf electrograph were taken in Portela, Lisbon,  
130 Portugal, which were analysed by Silva et al [17]. These were separated by fair weather and  
131 all weather and were characterised by a combination of anthropogenic and planetary cycles  
132 that contribute to the diurnal cycle, and also the purely anthropogenic weekly cycle.  
133 Weekdays showed a greater span of values than weekends, which indicated the effect of  
134 aerosol resistive loading of the atmosphere when traffic levels are higher. Lomb-Scargle  
135 periodograms indicated weekly, daily and half-daily cycles.

136 Subsequent analysis of the PG data set from Portela have shown correlation with aerosol due  
137 to the direct relationship between aerosol concentration and air conductivity [1], and a  
138 relationship between PG and pollutant gas concentrations, as both measurements are  
139 correlated with aerosol concentration [2].

140 A morning peak in the averaged diurnal cycle of the atmospheric PG was observed at a site in  
141 Israel [28] which was postulated to be due to a peak in aerosol concentration as a result of  
142 ground heating related uplift on aerosols. Atmospheric electrical measurements have been  
143 used to measure micro-meteorological features, for example Anisimov et al [29] used an array  
144 of electrical field mills in a site with low pollution levels to record the atmospheric PG at a  
145 sampling rate of 10 Hz. This approach delivered new insights in the turbulent transport of  
146 charge carriers (ions and charged aerosols) in the measurement location. A sunrise effect on  
147 artificially produced ions has been observed near high voltage power lines [30], where an  
148 increase in variability of PG measured by a field mill was shown to exist after sunrise; and a  
149 build-up of negative space charge overnight, which then dissipates after sunrise, was shown  
150 in PG measurements at a sub-urban UK Met Office site [5].

## 151 **2. Materials and Methods**

152

### 153 *2.1 Site descriptions*

154

155 Three different sites were chosen as monitoring locations for the atmospheric PG and local  
156 meteorology. Two were chosen in the City of Bristol, UK, and one in a rural location at  
157 Langford, North Somerset, UK. Pollutants, in particular aerosols, would be expected to be  
158 higher at the two urban sites, and any anthropogenic signal should be more apparent in these

159 than the rural Langford site. The urban sites were both on rooftops, one at the University of  
160 Bristol's School of Chemistry (SoC) and the other at the then-called at-Bristol Science Centre  
161 (AtB, since renamed We the Curious). The rural site is located 17 km away from the Bristol  
162 sites within the apiary of the University of Bristol's School of Veterinary Science in Langford  
163 (LVS). The two Bristol sites are 0.8 km apart (figure 1).

164



165

166

167 **Figure 1:** (a) map of England and Wales (b) Bristol and surrounding counties and (c) Bristol city centre showing  
168 the location of the two Bristol sites and the Langford site. Image credit: Google Earth, 08/08/2018.

169

## 170 2.2 Instrumentation

171

172 The atmospheric electric field can be measured using an electric field mill, which contains a  
173 rotating vane that induces a current alternately when the sensing vane is covered by a  
174 grounded vane, then uncovered and exposed to the atmospheric PG. The at-Bristol and  
175 Langford sites use a JCI 131F high frequency electric field mill, while the School of Chemistry  
176 roof site uses a JCI 131 field mill with a lower frequency response. The At-Bristol and Langford  
177 sites record at 10 Hz, which for this analysis was averaged to 1 s and 1 minute samples, the  
178 School of Chemistry site recorded samples at 1 s, also averaged to 1 minute. Local weather  
179 was recorded at 1 s by a Gill Maximet 501 integrated weather station measuring wind speed  
180 and direction, solar radiation, temperature, pressure and humidity and a Gill Maximet  
181 GMX100 to indicate rainfall at the Langford and at-Bristol sites. The GMX100 is a 0.08 mm  
182 resolution optical rain gauge, detecting the size and number of rain drops falling onto a glass  
183 dome and converting this to rainfall intensity  
184 (<http://gillinstruments.com/products/anemometer/maximet-compact-weather-stations.html>). The  
185 School of Chemistry site used a Gill Maximet GMX500 measuring wind speed and direction,



186 temperature, humidity and pressure, and also contained occasional aerosol measurements  
187 using a TSI 3010 Condensation Particle Counter.

188

### 189 *2.3 Instrument locations*

190

191 The field mill and weather stations on the University of Bristol rooftop were placed on a 1.5  
192 m stand, the roof was 30 m from the ground on the South side and 22 m from the ground on  
193 the North side, as the building is on a hill. The rooftop location is shielded by a larger building  
194 and smaller buildings surrounding the measurement location, and therefore the weather  
195 conditions measured at this site are locally affected by the surroundings, in particular the  
196 wind speed which is affected by street channelling and cannot be assumed to be  
197 representative of the weather conditions in Bristol as a whole. The instruments on top of the  
198 at-Bristol science centre were mounted on 2 m poles on the building edge, but unlike the  
199 Bristol University site, they are not sheltered by other buildings. The building height is 15 m  
200 above ground near the harbourside, in a low lying part of Bristol. The Langford Apiary site is  
201 not a rooftop site, but in a small fenced area, the instruments are mounted on two separate  
202 2 m stands near to some bee hives. A large tree does exist ~5 m from the field mill which may  
203 affect the overall value of atmosphere PG to an extent that may be seasonal, and the  
204 instruments were close to some wind shields erected to protect the beehives nearby, but the  
205 wind shields were shorter in height than the field mill and weather stations. These positions  
206 are summarised in table 1.

207

208 **Table 1:** Instrument locations

Site	Building Height	Instrument Height	Latitude	Longitude
SoC	26 m	1.5 m	51.4570 deg	-2.6000 deg
AtB	15 m	2 m	51.4506 deg	-2.6008 deg
LVS	NA	2 m	51.3467 deg	-2.7798 deg

209

210

211 *2.4 Field calculations*

212

213 An electric field mill on a conducting pole can act as a potential probe, but will enhance the  
214 field due to its own geometry. The field measured at the instrument surface ( $E_f$ ) is affected as  
215 a function of the field mills effective diameter,  $d$ , and the height above ground  $h$ . The  
216 calculation to estimate the atmospheric PG at the field mill sites is given in Eq. (1) [31].

217

$$218 \quad PG = E_f d / h \quad (1)$$

219

220 The three sites chosen for these instruments are not ideal sites for absolute values of PG as  
221 building geometries and other conducting structures can distort the field enhancing the PG at  
222 the measurement point. However, the enhancement is a function of the geometry and, if the  
223 geometry of the site does not change, then a simple form factor can provide a corrected value  
224 of PG as if the measurement were taken on a flat plain, but for the current study, corrected  
225 values were not used.

226

227 *2.5 Limitations of the data set*

228

229 There are two limitations to the work presented here that could not be overcome in the  
230 current study. First, the data set is not long enough for conclusions to be drawn on seasonal  
231 or annual effects, and second the data is presented as actual field values and not corrected  
232 for the presence of buildings and height above ground. It was not possible to collect more  
233 data from all three sites running simultaneously (equipment availability) and therefore the  
234 comparison of sites, which was an aim of the study, can only be undertaken with the data  
235 available. The data set does allow subsets of the data to be analysed to investigate specific  
236 questions regarding aerosol content and meteorology.

237

238 It was also not possible to make measurements using, for instance, a passive wire antenna or  
239 calibrated field mill, on a nearby flat area of ground to measure the effects of building  
240 distortion due to the malfunction of two of the three field mills in the study. While corrected  
241 values would be required if these data were used to estimate charges overhead in clouds, for  
242 example, the shape of the time series is enough to discern much about ion-aerosol

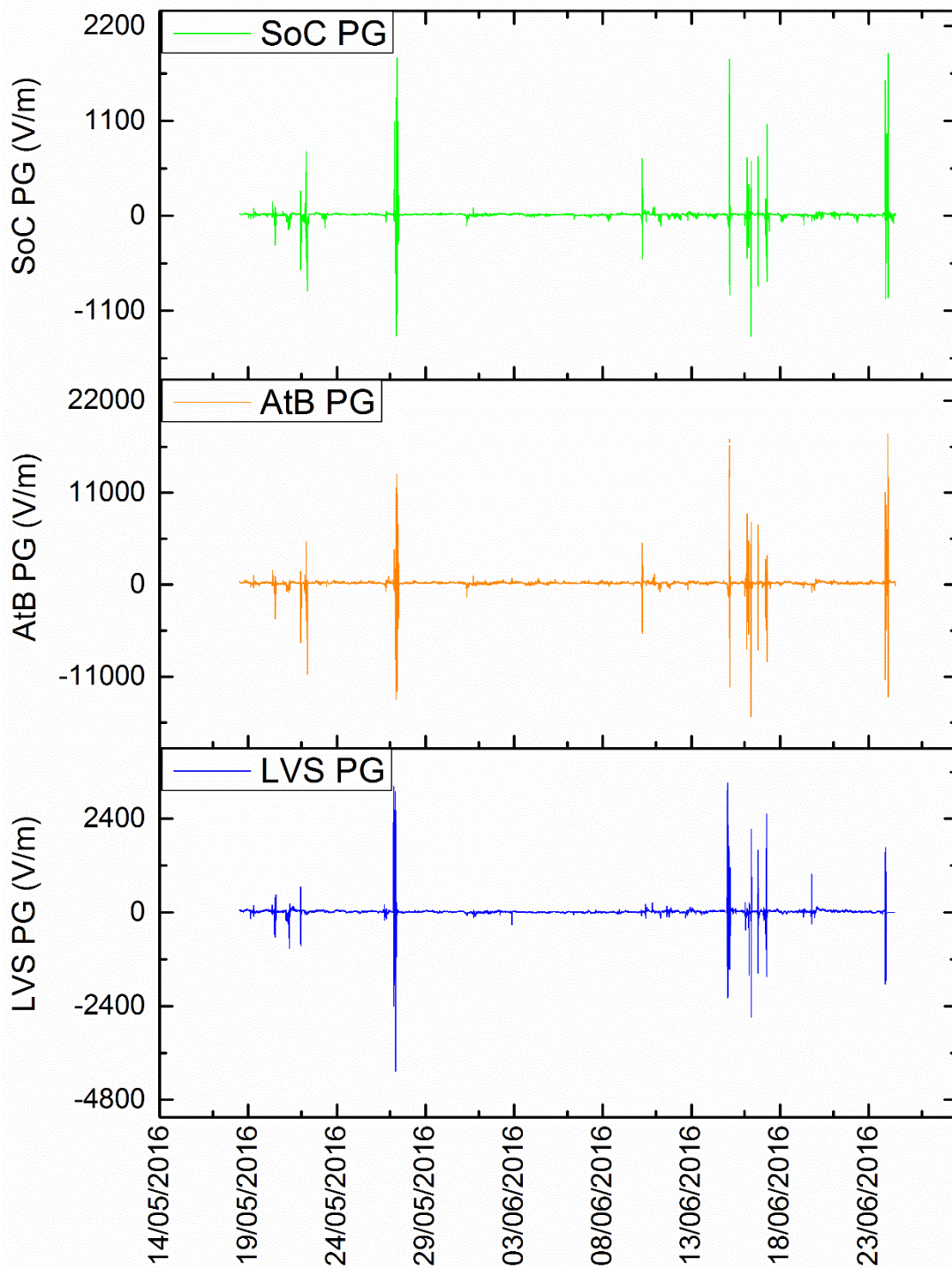
243 interactions, and other factors affecting ground-based measurements of PG in urban and rural  
244 settings. Comparison of the shape of the time series and distributions of the measured fields  
245 enable differences in weather effects and aerosol loading to be investigated.

246

### 247 **3. Results**

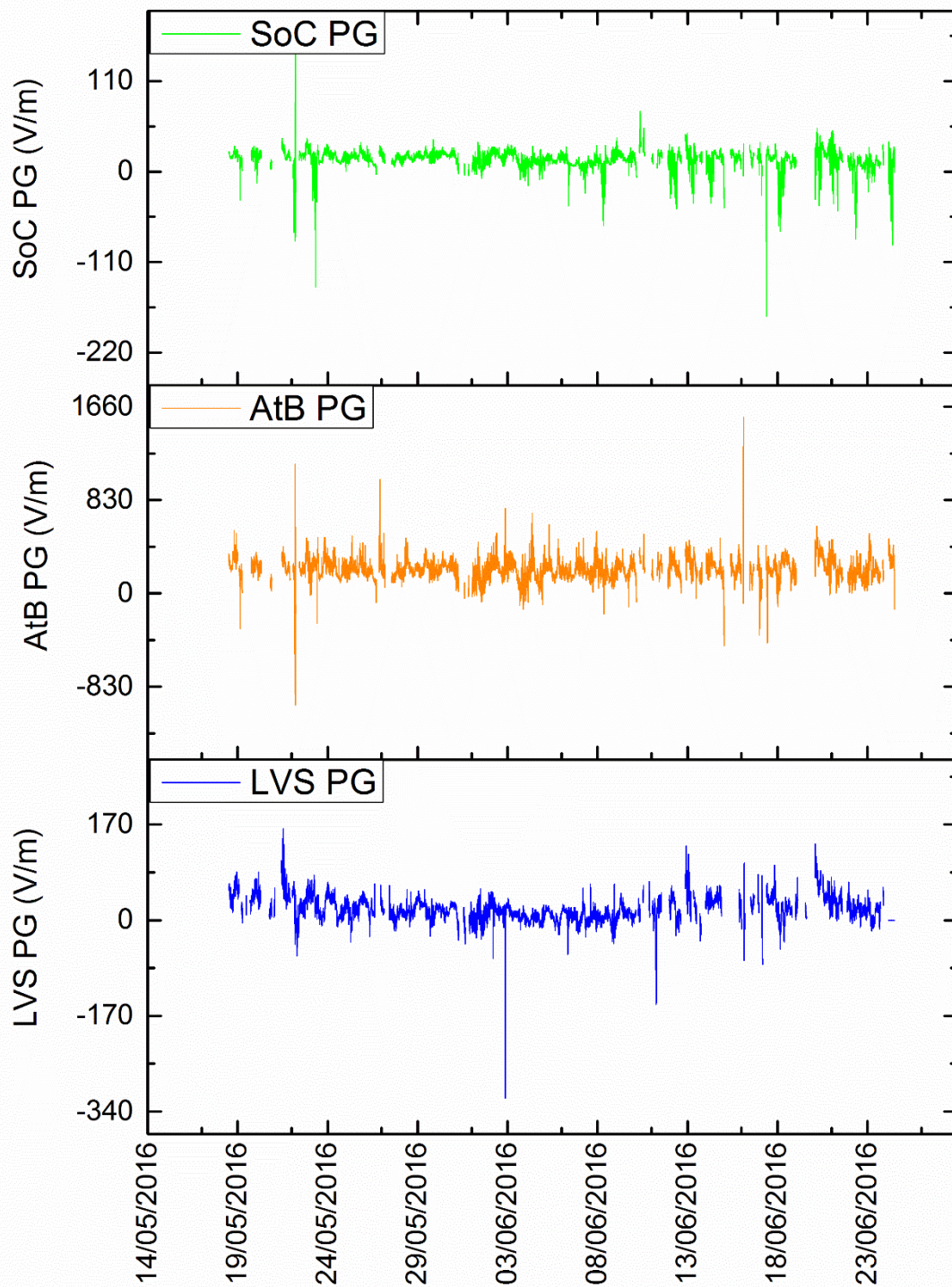
#### 248 *3.1 Time series of whole data set*

249 The data collected at all three sites are represented as time series in figure 2, showing the  
250 largest variations of PG present in disturbed weather. To concentrate on fair weather fields,  
251 any data during and 60 minutes before the onset and after the finish of rain as measured on  
252 the GMX100 were removed. The SoC site did not have an instrument to measure rain and so  
253 used the same measurement as AtB. The resulting time series is shown in figure 3 and shows  
254 a much more stable field, with the rain removed, though some periods of disturbed PG remain  
255 implying that rainfall alone is not enough of an indication of fair weather fields.



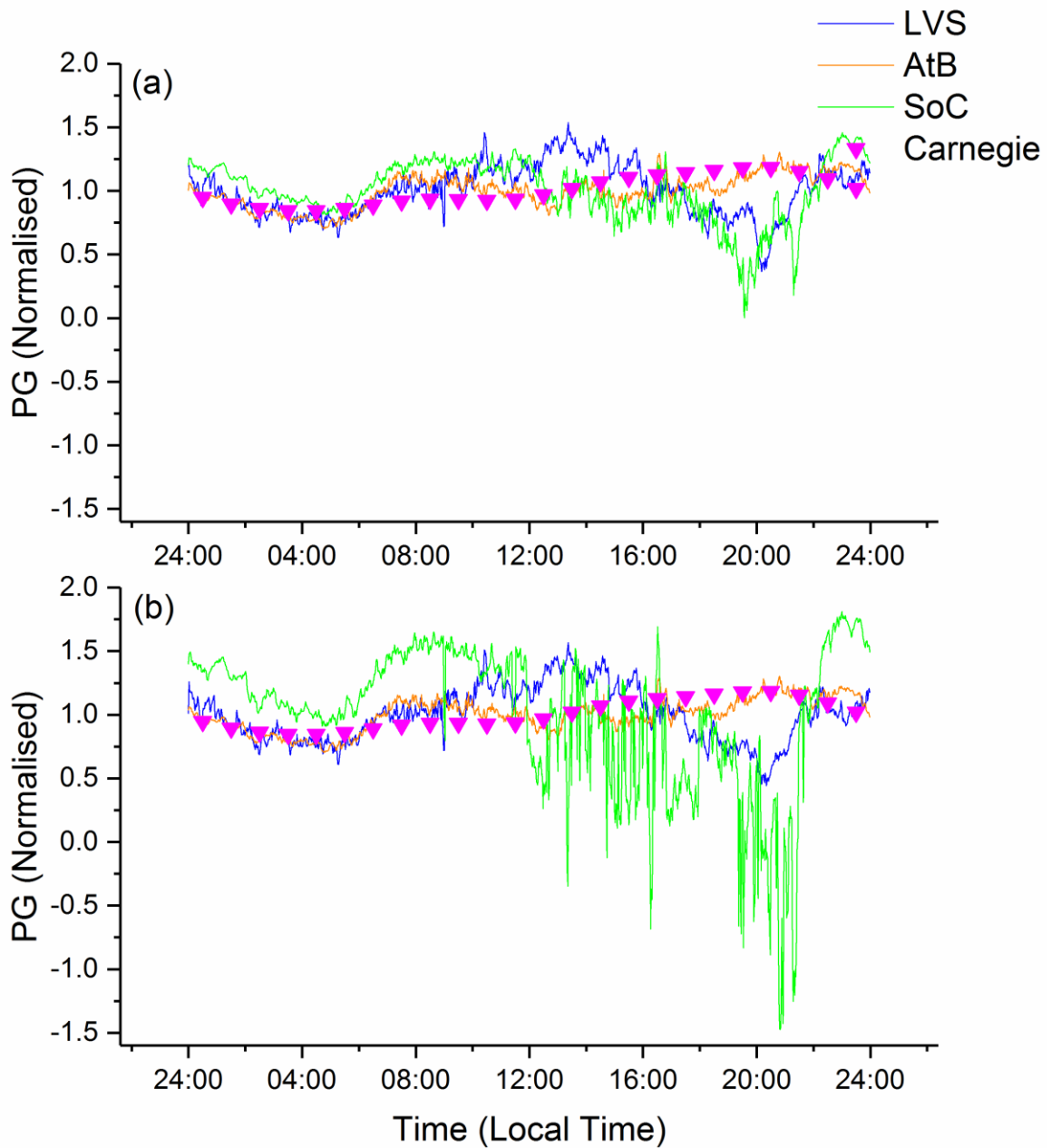
256

257 **Figure 2:** Time series of atmospheric PG measured at the Langford Vet School rural site (LVS, blue), the At-  
 258 Bristol Science Museum (AtB, orange) and the School of Chemistry in Bristol (SoC, green).



259

260 **Figure 3:** Time series of atmospheric PG measured at the Langford Vet School rural site (LVS, blue), the At-  
 261 Bristol Science Museum (AtB, orange) and the School of Chemistry in Bristol (SoC, green) with data removed  
 262 during and for one hour before and after rainfall.



264

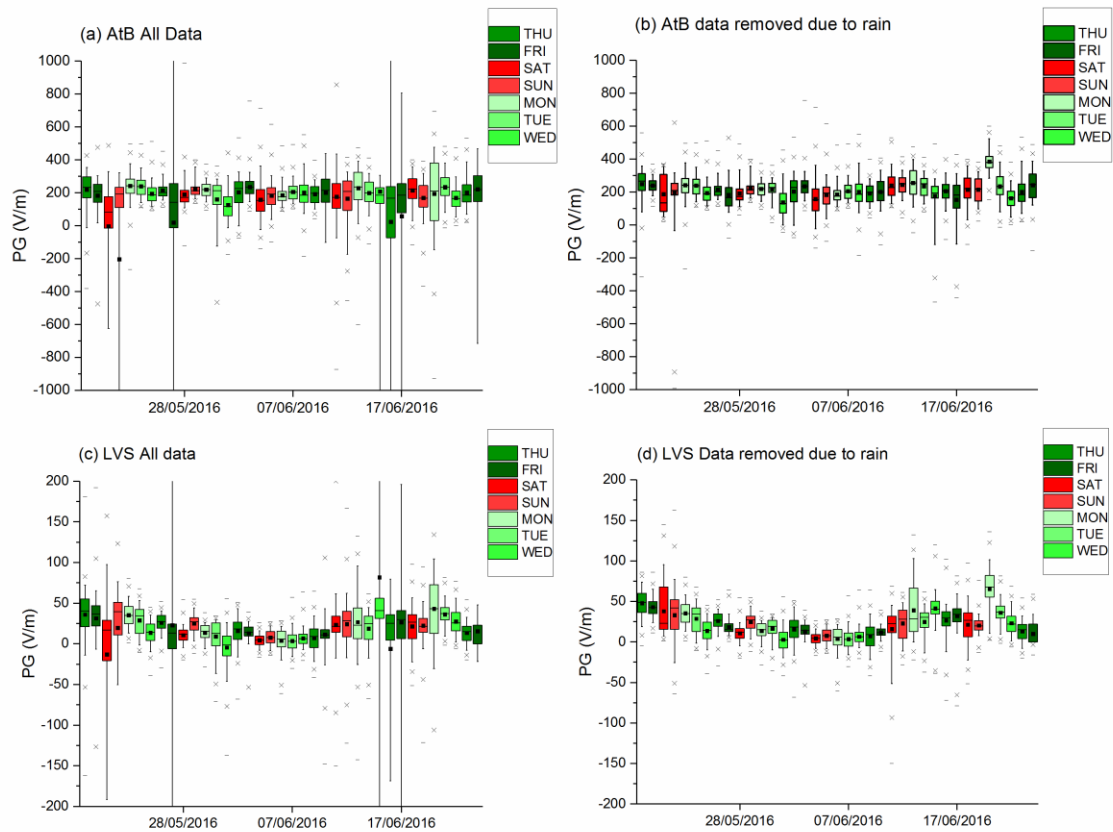
265 **Figure 4:** Averaged daily cycle (a) when rain is removed one hour before, after and during rainfall, and (b) with  
 266 five days of extreme fields also removed. Carnegie curve data reproduced from [12].

267 The daily average curve was calculated from the data set with the rain removed and are  
 268 plotted against the Carnegie curve [12] (local time) in figure 4(a), normalised to their own  
 269 mean. We might expect the urban fields to show peaks at rush hour to correspond to the



270 increased aerosol concentration, and there may be peaks at 8 am and 5 pm (local time) in the  
271 AtB trace, but, no such peak was evident at the SoC site. It is also notable that the three sites  
272 correlate best to each other and to the Carnegie curve overnight when conditions are calmer  
273 on average and aerosol concentrations within the city are lower. However, the large  
274 variations in field at the LVS and SoC sites in the afternoon are sufficient to mask any aerosol  
275 loading effect. Removal of five days of data that show large extremes of PG due to disturbed  
276 weather (22/05/2016, 23/05/2016, 03/06/2016, 16/06/2016, 17/06/2016) increases the  
277 variability of the normalised data at the SoC site (figure 4(b)) comparatively to the other data  
278 sets, as that variability is now larger in comparison to the baseline. As this is the only site  
279 where rain incidence is not recorded in the same location, it may be due to local variation in  
280 rainfall, but large differences in weather conditions over neighbourhood scales is unlikely. It  
281 may also be the case that the relative increase in PG at AtB relative to LVS and SoC between  
282 16 and 22 hours could be due to local aerosol loading at the urban site given its close proximity  
283 to a busy road.

284 To show the variation with each day, figure 5 shows boxplots for every day within the study  
285 site for the two sites (AtB and LVS). They represent the 95<sup>th</sup>, 75<sup>th</sup>, 50<sup>th</sup>, 25<sup>th</sup> and 5<sup>th</sup> percentiles  
286 of the PG within that day and show the great variability within days and day to day that can  
287 be present. The most electrically disturbed days are shown by the highest spread of values in  
288 both sites. If data are removed one hour before and after recorded rainfall, the box plots show  
289 less extreme values (figure 6) and allow for better comparison between the two sites, but  
290 highly variable days are still evident.

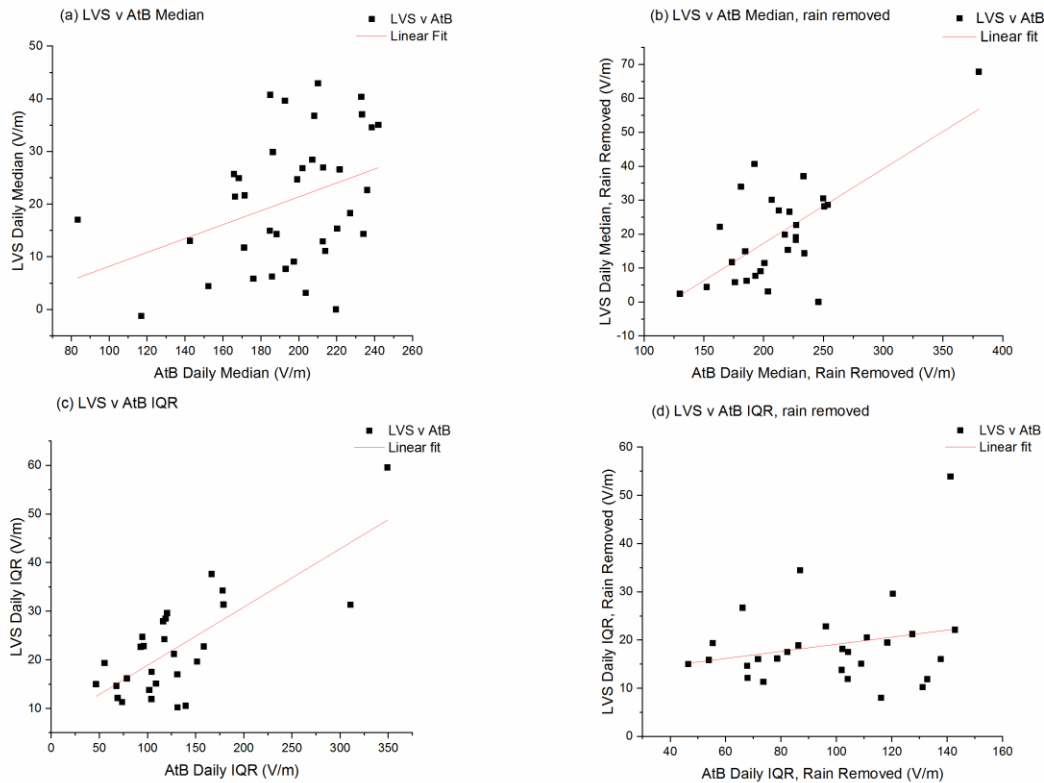


291

292 **Figure 5:** Box and whisker plots of (a) the AtB site in Bristol with all data and (b) data removed one hour  
 293 before, after and during rainfall and (c) the LVS site with all data and (d) data removed one hour before, after  
 294 and during rainfall. Boxplots show 95<sup>th</sup>, 75<sup>th</sup>, 50<sup>th</sup>, 25<sup>th</sup> and 5<sup>th</sup> percentiles of PG values in each day.

295 Scatter plots of both the mean and the interquartile range of the daily PG values were made  
 296 to test similarities in the urban and rural sites. Correlations were tested using a Pearson  
 297 correlation one tailed test. The daily median had a Pearson correlation coefficient  $r = 0.36$   
 298 with all data, but  $r = 0.68$  when rain data was removed, while conversely the interquartile  
 299 range was better correlated with all data ( $r = 0.76$ ) than when rain data was removed ( $r =$   
 300  $0.23$ ). The better correlation in daily median when rain data is removed suggests that global  
 301 background fields do have a degree of similarity with the two sites, but that this is masked in  
 302 disturbed weather, whereas the greater correlation in interquartile range when disturbed  
 303 weather is included shows that the most disturbed weather affects both sites at the same  
 304 day.



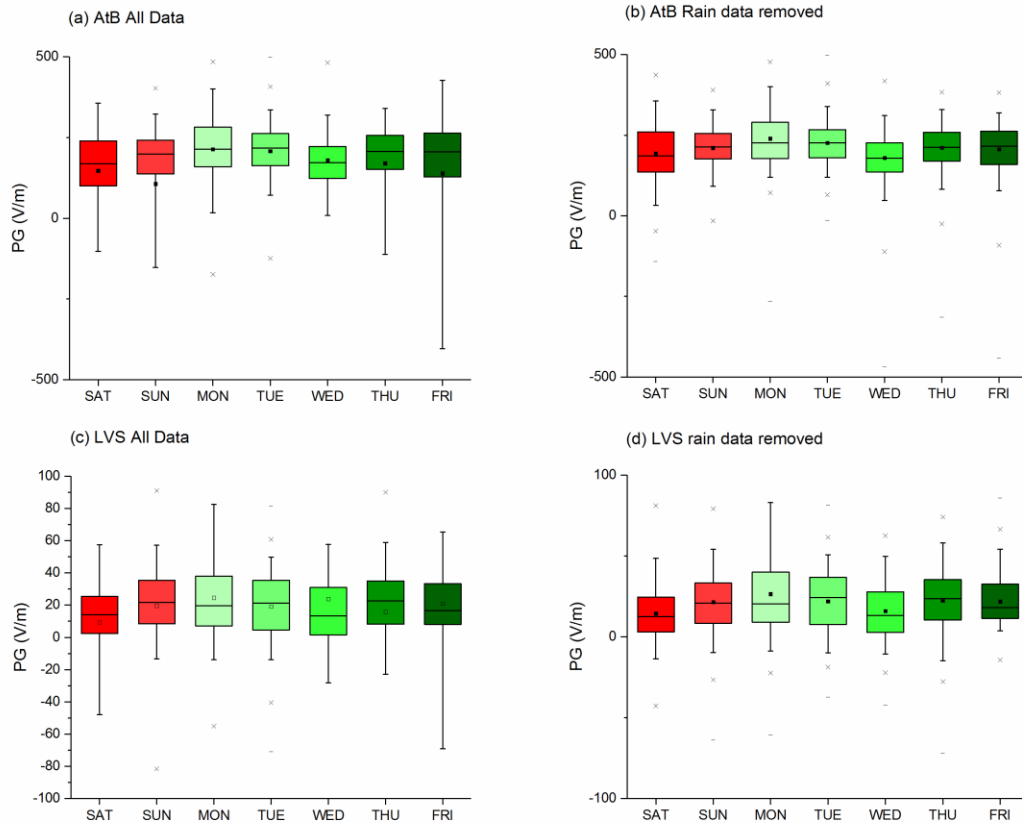


305

306 **Figure 6:** Scatter plots comparing (a) daily PG median and (b) interquartile range values between the rural LVS  
 307 site and the urban AtB site for all values, and for (c) median and (d) interquartile range with data removed  
 308 during and one hour before and after rainfall.

309 An attempt to average each day to ascertain whether weekends and weekdays were  
 310 noticeably different did not show any clear weekend / weekday difference (figure 7), the  
 311 highest and most variable values were on Monday, in both sites. This may be due to the  
 312 disturbed weather on the 20<sup>th</sup> June having an undue influence, and so therefore there is not  
 313 enough statistical power in this dataset to see any predicted weekend / weekday differences  
 314 caused by higher levels of aerosol present as meteorological events mask any potential effect.  
 315 The size of the data set is not sufficient not investigate seasonal effects or long term trends  
 316 within the data series, but the series includes 37 days of data from three unique sites in a  
 317 variety of weather conditions, including some extreme weather events. Examples of high and  
 318 low aerosol days, and of disturbed weather events can be investigated to demonstrate the  
 319 effect of aerosol in urban measurements, and the distance scale of atmospheric PG changes.

320



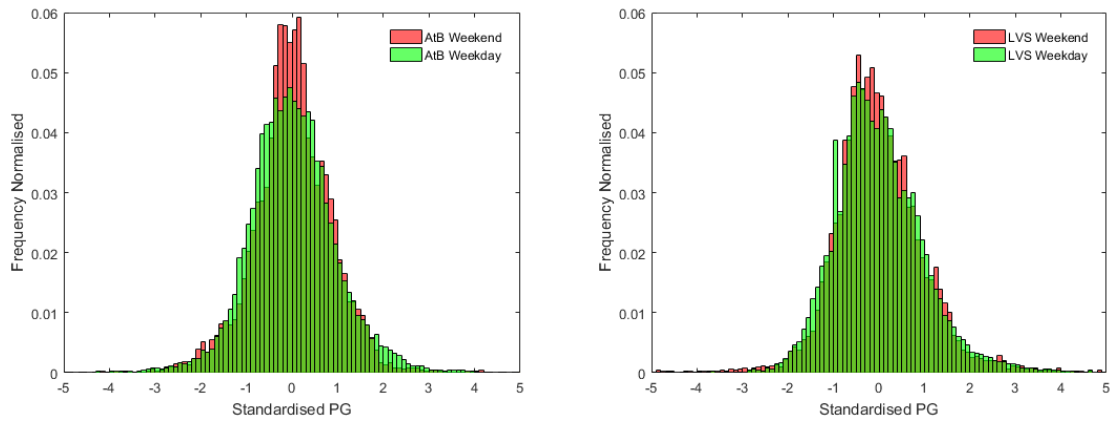
321

322 **Figure 7:** Box plots for PG values for all data separated by day of the week, showing 95<sup>th</sup>, 75<sup>th</sup>, 50<sup>th</sup>, 25<sup>th</sup> and 5<sup>th</sup>  
 323 percentiles of PG values in the rural LVS site and the urban AtB site for all values, data removed during and one  
 324 hour before and after rainfall.

### 325 3.2 Fair weather effects of aerosol

326 PG levels are known to be affected by aerosol concentrations by increasing the resistivity of  
 327 the air, to test whether this effect shows a difference in aerosol levels that could be present  
 328 at weekends and weekdays, a histogram was created of the 1 minute averages of PG in both  
 329 the urban AtB site and the rural LVS site separated by weekend and weekday (data discarded  
 330 during and 60 minutes before and after rain).

331



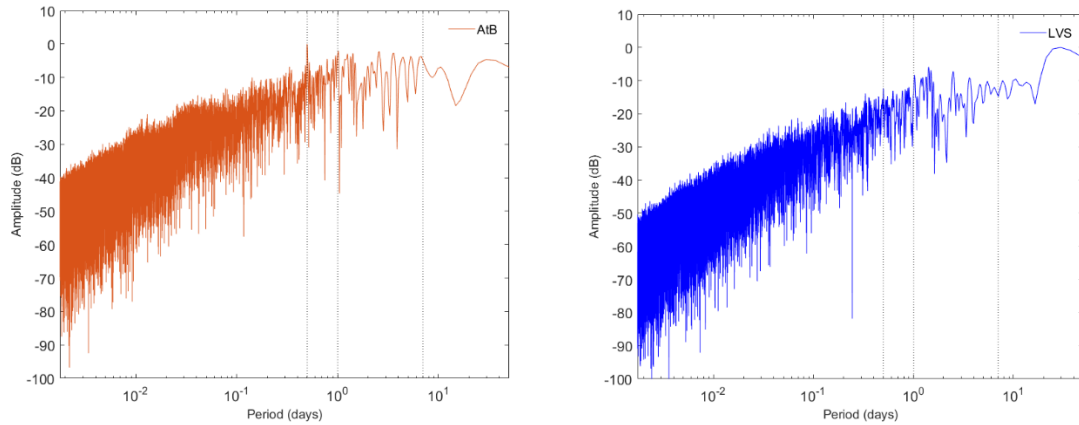
332

333 **Figure 8:** Normalised histograms of the weekday (green) and weekend (red) PG measurements for the LVS  
 334 rural site and AtB urban site with data removed during and one hour before and after rainfall.

335 All plots exhibit a normal distribution. There is a visual difference in histogram shape in the  
 336 histograms at AtB, with a narrower distribution during the weekend (when aerosol content  
 337 would be lower). However, Kolmogorov-Smirnov tests were run, and no statistical difference  
 338 was found between the distributions of weekend and weekday distributions of PG ( $p < 0.01$   
 339 for both LVS and AtB sites).

340 Lomb-Scargle periodograms allow the frequency spectrum to be calculated in interrupted  
 341 data sets by estimating the frequency spectrum from a least-squares fit of the sinusoids [32,  
 342 33]. The urban AtB site and the rural LVS site were compared. Weekends at an urban site have  
 343 lower traffic and therefore lower air pollution, consequently a weekly 7-day cycle may be  
 344 evident in the AtB site, but not in the LVS site, whereas the 24 cycle is seen in both sites (Figure  
 345 9), but a larger data set would be required to have any confidence in a seven day cycle. There  
 346 is a clear half day cycle evident in the AtB site which would account for the double diurnal  
 347 traffic signal, rather than the single daily cycle that the Carnegie curve shows.

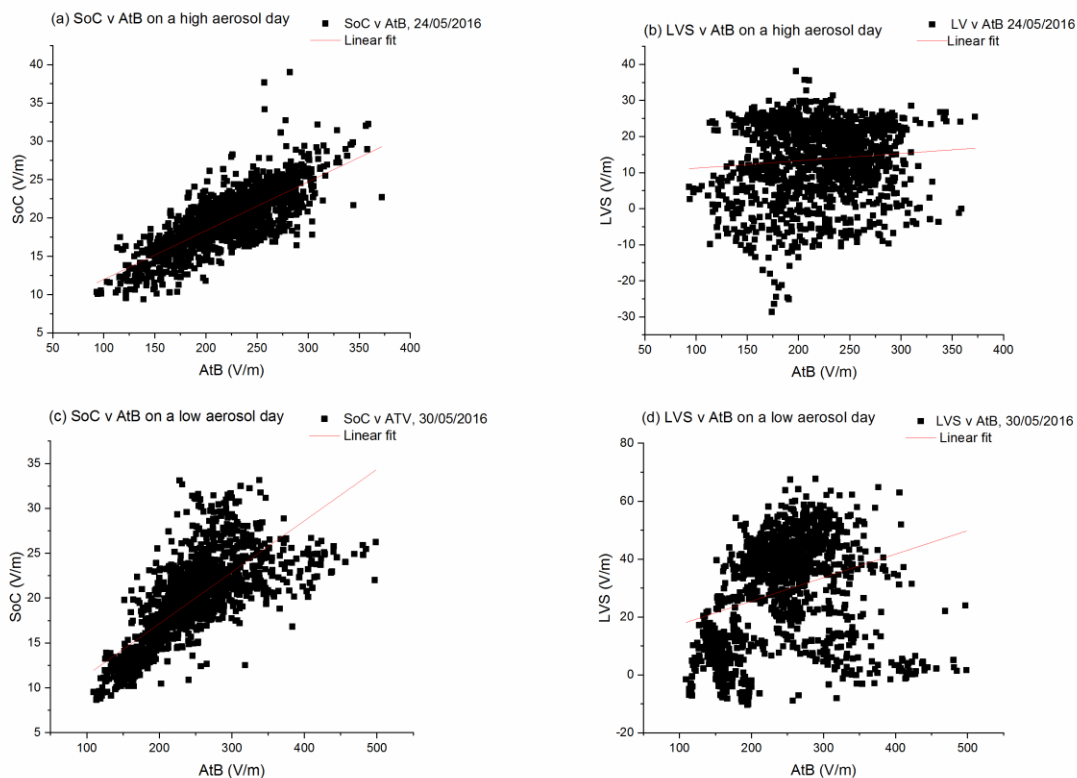
348



349

350 **Figure 9:** Lomb Scargle periodograms of 1 minute average PG measured at the AtB urban and LVS rural sites,  
 351 dashed vertical lines represent a half-day, full-day and weekly cycle.

352 Given that aerosol content has been shown to have an effect on atmospheric PG in previous  
 353 studies, the correlation between PG at the two Bristol sites was investigated on a weekday  
 354 chosen with high aerosol content and a public holiday with low aerosol content measured at  
 355 the SoC site using a TSI 3010 CPC. Figure 10 shows that the correlations between the two sites  
 356 are similar on both the high and low aerosol days, with good correlation in the Bristol sites  
 357 and poor correlation with the Bristol and Langford sites; a Pearson correlation coefficient  $R =$   
 358  $0.76$  and  $R = 0.77$  between AtB and SoC on the high and low aerosol days respectively, and  $R =$   
 359  $0.31$  and  $R = 0.09$  between AtB and LVS ( $p > 0.99$ ).



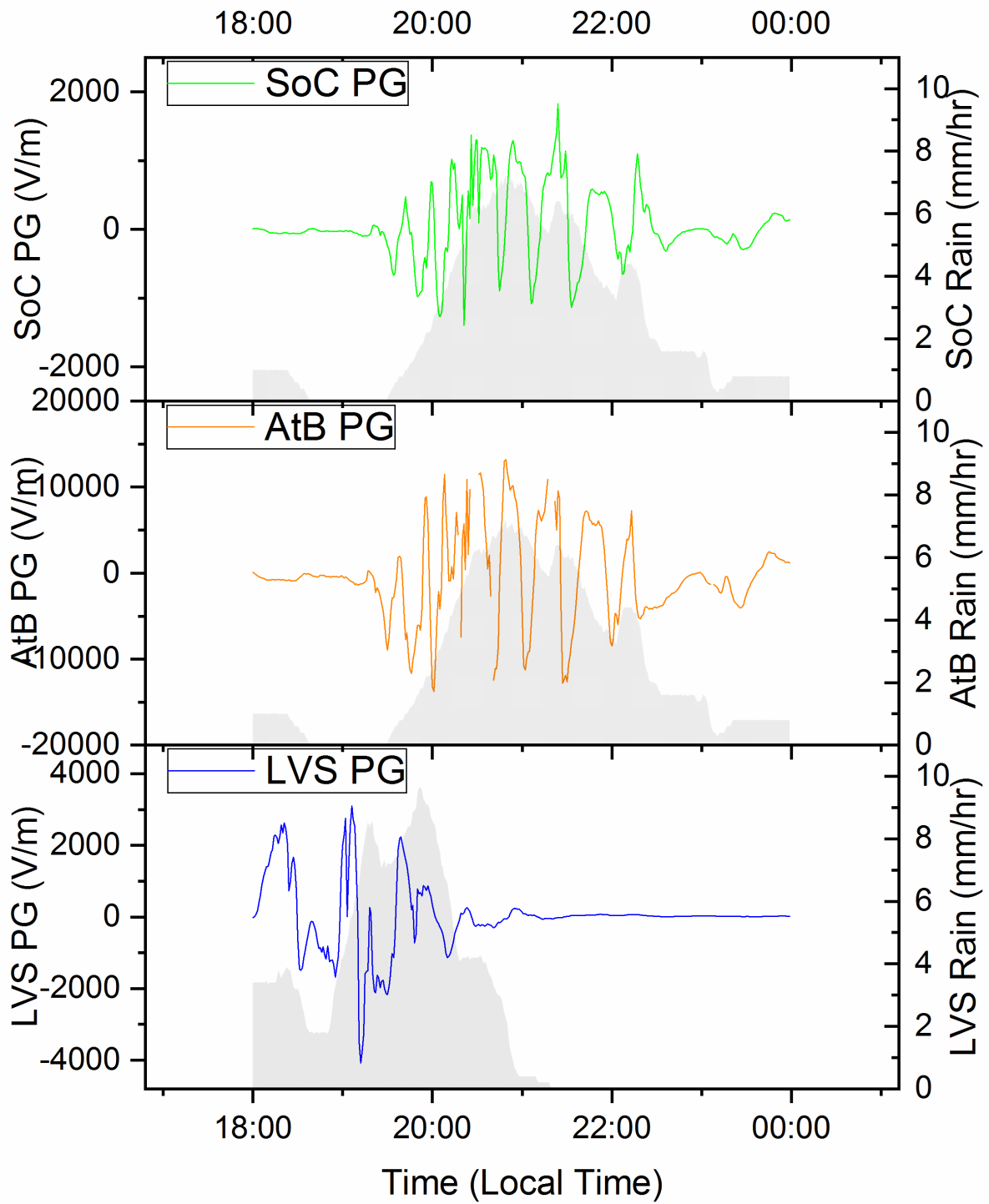
360

361 **Figure 10:** Correlations between (a) the AtB and SoC site and (b) the SoC and LVS site on 24/05/2016, a day with  
 362 high aerosol content and between (c) the AtB and SoC site and (d) the SoC and LVS site on 30/05/2016, a day  
 363 with low aerosol content)

364 *3.3 Distance scale of disturbed weather effects*

365 While the fair-weather fields could show the effect of traffic in an urban environment, any  
 366 aerosol related local effects can be masked by the large changes in field shown by disturbed  
 367 weather. One example of a disturbed weather day is presented here. A storm passed both  
 368 Langford and Bristol on the 27<sup>th</sup> May 2016 exhibiting typical field inversions and large field  
 369 values as indicated in the box plot in figure 5.

370 Figure 11 shows the field values for a 6 hour extract at the three sites, there were storms  
 371 travelling from the South East, and the storm is shown passing Langford at 18:00 and Bristol  
 372 at 19:30. The alternating polarity reversals is characteristic of multicellular convection, with a  
 373 good agreement between both Bristol sites showing that the storm affects PG values over a  
 374 city scale.



375

376 **Figure 11:** The passage of a storm showing disturbed weather at the (a) AtB, (b) SoC and (c) LVS sites. Shaded  
 377 grey profile graphs show rainfall recording.

378

379 **4. Conclusions**

380 The measurements from these three sites show consistency with previous findings on  
381 anthropogenic aerosol related effects on PG, and in the extent to which disturbed weather  
382 affects local PG measurements. It has also allowed new insights into the length scales to which  
383 these effects occur, and has shown the use of precipitation alone as an indicator of electrically  
384 disturbed weather to be inadequate.

385 Having two PG measurements within a city allowed an opportunity to test whether increased  
386 aerosol concentration within a city would increase localised effects on PG by reducing the  
387 correlation between both sites. Selecting a high and low aerosol concentration day and  
388 comparing the Pearson correlation provided a first test, but no difference was found. During  
389 disturbed weather, the field inversions caused by charge carriers overhead were temporally  
390 similar in both urban sites, but different in the rural site several km away. These first tests  
391 have shown that the PG fluctuations measured at one roof top site in the city can be assumed  
392 to represent that of the surrounding 1 km, though absolute values will be affected by local  
393 geometry. The example of a thundercloud passing overhead showing similar fields at the two  
394 urban sites shows that this similarity holds in disturbed weather. Further tests should look at  
395 street level and roadside measurements to measure whether newly generated charges and  
396 particles from vehicles provide greater local distortions to the global field.

397 It is well known that rain and storm clouds cause large disturbances in the atmospheric PG,  
398 which is why researchers interested in global properties of the atmospheric electric field will  
399 often remove disturbed weather. While a general consensus on how to establish what is 'fair  
400 weather' has not yet been reached, it is usually assumed to mean clear skies with no  
401 precipitation and low wind speeds, though recent efforts have been made towards a  
402 standardised definition that include the removal of very low ( $< 1 \text{ ms}^{-1}$ ) wind speeds, and a  
403 more robust criteria on cloud cover [13]. In the present study, cloud cover was not measured  
404 and cannot be used to identify disturbed weather. While removing data one hour either side  
405 of rain removed most disturbed weather, large fluctuations of field on stormy days still  
406 persisted, and so rain measurements alone are not sufficient to identify fair weather.

407 **Acknowledgements**

408 This work was funded by Leverhulme Trust Research Project Grant [Grant number RPG-2014-  
409 102], National Environment Research Council [Grant number NE/K01501X/1] and the  
410 Biotechnology and Biological Sciences Research Council [Grant number BB/M011143]. We  
411 would like to thank the staff of the Langford site and We the Curious for assistance in creating  
412 and maintaining the monitoring sites. Data from these sites is stored in the GloCAEM  
413 database, the GloCAEM data catalogue can be found at:  
414 <http://catalogue.ceda.ac.uk/uuid/bffd0262439a4ecb8fadf0134c4a4a41>.

415

## 416 **References**

417 [1] Silva, H.G., Conceição, R., Wright, M.D., Matthews, J.C., Pereira, S.N., and Shallcross, D.E.  
418 2015. Aerosol hygroscopic growth and the dependence of atmospheric electric field  
419 measurements with relative humidity. *J. Aerosol Sci.* 85, 42-51.

420 [2] Silva, H.G., Conceição, R., Khan, M. A. H., Matthews, J.C., Wright, M.D, Collares-Pereira,  
421 S.N. and Shallcross, D.E. 2016b. Atmospheric Electricity as a proxy for Air Quality: relationship  
422 between Potential Gradient and Pollutant Gases in an Urban Environment. *J. Electrostat.* 84,  
423 32-41.

424 [3] Aplin, K. L. 2012 Smoke emissions from industrial western Scotland in 1859 inferred from  
425 Lord Kelvin's atmospheric electricity measurements *Atmos. Environ.* 50 373-376.

426 [4] Harrison R. G. 2006. Urban smoke concentrations at Kew, London, 1898 – 2004 *Atmos.*  
427 *Environ.* 40 3327 – 3332.

428 [5] Piper, I. M. and Bennett, A. J. 2012. Observations of the atmospheric electric field during  
429 two case studies of boundary layer processes. *Environ. Res. Lett.* 7 014017.

430 [6] Harrison, R. G., Nicoll K. A., Marlton, G. J., Ryder, C. L. and Bennett, A. J. 2018. Saharan  
431 dust plume charging observed over the UK. *Environ. Res. Lett.* 13 054018.

432 [7] Clarke, D, Whitney, H., Sutton, G. and Robert, D. 2013. Detection and learning of floral  
433 electric fields by bumblebees. *Science*, 340, 66-69.



- 434 [8] Morley, E.L. and Robert, D. 2018. Electric fields elicit ballooning in spiders. *Current Biology*,  
435 28 (14), 2324-2330.
- 436 [9] Wilson C.T.R., 1920. Investigations on lightning discharges and on the electric field of  
437 thunderstorms *Phil. Trans. Roy. Soc. Lond. A* 221, 73-115.
- 438 [10] Anisimov, S. V. and Mareev, E. A. 2008. Geophysical studies of the global electric circuit.  
439 *IZV-Phys. Solid Earth.*, 44 (10), 760-769.
- 440 [11] Chalmers, J. A. *Atmospheric Electricity* 2nd Ed. Pergamom Press, Oxford 1963.
- 441 [12] Harrison, R. G. 2013 The Carnegie Curve. *Surv. Geophys.* 34 (2) 209-232.
- 442 [13] Harrison, R.G. and Nicoll, K.A., 2018. Fair weather criteria for atmospheric electricity  
443 measurements. *J. Atmos Solar-Terr. Phys.* 179, 239-250.
- 444 [14] Muir, M. S. 1977 Atmospheric electric space-charge generated by the surf. *J. Atmos. Terr.*  
445 *Phys.* 39 1341–1346.
- 446 [15] Matthews, J.C., Buckley, A.J., Wright, M.D. and Henshaw, D.L., 2012. Comparisons of  
447 ground level measurements of ion concentration and potential gradient upwind and  
448 downwind of HV power lines in corona. *J. Electrostat.* 70 (4) 407-417.
- 449 [16] Israelsson, S., Lelwala, R. 1999. Space charge density measurements downwind from a  
450 traffic route *Atmos. Res.*, 51 (3–4), 301-307.
- 451 [17] Silva, H. G., Conceição, R., Melgão, M., Nicoll, K., Mendes, P. B., Tlemcani, M., Reis, A. H.  
452 and Harrison, R. G. 2014. Atmospheric electric field measurements in urban environment and  
453 the pollutant aerosol weekly dependence. *Environ. Res. Lett.* 9, 114025.
- 454 [18] Latha, K. M., Bennett, A. J., Highwood, E. J. and Harrison, R. G. 2008. Retrieval of global  
455 atmospheric electrical activity at a polluted urban site. *J. Phys: Conf Ser.* 142 (1) 012046.
- 456 [19] Rycroft, M. J., Nicoll, K.A., Aplin, K. L. and Harrison, R.G. 2012. Recent advances in global  
457 electric circuit coupling between the space environment and the troposphere. *J. Atmos. Solar-*  
458 *Terr. Phys.* 90-91, 198-211.

- 459 [20] Nicoll, K. A., 2014. Space weather influences on atmospheric electricity. *Weather*, 69 (9),  
460 238-241.
- 461 [21] Rycroft, M. J., Israelsson, S. and Price, C. 2000. The global atmospheric circuit, solar  
462 activity and climate change. *J. Atmos. Solar-Terr. Phys.* 62, 1563 – 1576.
- 463 [22] Bennett, A. J and Harrison, R. G. 2007. Atmospheric electricity in different weather  
464 conditions. *Weather*. 62 (10) 277-283.
- 465 [23] Bracken, T. D., Senior, R. S. and Bailey, W. H. 2005. DC electric fields from corona-  
466 generated space charge near AC transmission lines. *IEEE Trans. Power Deliv.*, 20 (2), 1692-  
467 1702.
- 468 [24] Blanchard, D. C. 1966 Positive space charge from sea. *J. Atmos. Sci.* 23(5) 507–515.
- 469 [25] Lopes, F., Silva, H. G., Salgado, R., Potes, M., Nicoll, K. A. and Harrison, R. G. 2016.  
470 Atmospheric electrical field measurements near a fresh water reservoir and the formation of  
471 the lake breeze. *Tellus A* 68 31592
- 472 [26] Jayaratne E. R., Ling, X. and Morawska, L. 2015. Comparison of charged nanoparticle  
473 concentrations near busy roads and overhead high-voltage power lines. *Sci. Tot. Environ.* 526  
474 14-18.
- 475 [27] Silva, H.G., Lopes, F. M., Pereira, S., Nicoll, K., Barbosa, S. M., Conceição, R., Neves, S.,  
476 Harrison, R. M. and Collares-Pereira, S.N. 2016a. Saharan dust electrification perceived by a  
477 triangle of atmospheric electricity stations in Southern Portugal. *J. Electrostat.* 84, 106-120.
- 478 [28] Yaniv, R., Yair, Y., Price, C. and Katz, S. 2016. Local and global impacts on the fair-weather  
479 electric field in Israel. *Atmos. Res.* 172, 119-125.
- 480 [29] Anisimov, S. V., Galichenko, S. V. and Shikhova, N. M. 2014. Space charge and aroelectric  
481 flows in the exchange layer: An experimental and numerical study. *Atmos. Res.* 135-136, 244-  
482 245.
- 483 [30] Matthews, J. C. 2012. Diurnal variations of atmospheric potential gradient disruption  
484 near to high voltage power lines. *J. Atmos Solar-Terr. Phys.* 77, 235-240.

485 [31] Chubb, J. N. 2006. User Manual: JCI 131 Electrostatic Fieldmeter, UM131, Issue 9.  
486 <http://www.infostatic.co.uk/UM/UMJCI131.pdf> Accessed 04/04/2018.

487 [32] Lomb, N. R. 1976. Least-squares frequency analysis of unequally spaced data. *Astrophys.*  
488 *Space Sci.* 39 447–462.

489 [33] Scargle, J. D. 1982. Studies in astronomical time series analysis: II—statistical aspects of  
490 spectral analysis of unevenly spaced data. *Astrophys. J.* 263 835.

491

492

493